OnLine Journal of Biological Sciences

Original Research Paper

Mechanism Analysis of Artemisinin and Artesunate as Lung Cancer Therapy Agents Through in Silico Method

[1]Didik Harmoko, [2]Vivitri Dewi Prasasty and [1]Adi Yulandi

[1]Faculty of Biotechnology, Atma Jaya Catholic University of Indonesia, Cisauk, Tangerang, Banten, Indonesia
[2]Department of Biology, Faculty of Biology and Agriculture, Universitas Nasional, Jakarta, Indonesia

Article history
Received: 23-07-2023
Revised: 20-11-2023
Accepted: 22-01-2024

Corresponding Author:
Adi Yulandi
Faculty of Biotechnology,
Atma Jaya Catholic University of Indonesia, Cisauk,
Tangerang, Banten, Indonesia
Email: adi.yulandi@atmajaya.ac.id

Abstract: Several *in vitro* studies have focused on the ability of artemisinin and its derivatives to suppress lung cancer cells, but there are still many biological processes and mechanisms, such as the interactions between the active compounds (ligands) and receptors that are not well understood and require further research. Drug targeting for lung cancer will be more precise and the inhibition of cancer cell proliferation will be increased as a result of understanding the mechanism of interaction between artemisinin and its derivatives with lung cancer receptors. Currently, there are no studies that report the interaction between artemisinin and its derivatives with the PARP1 receptor. The results of this study will offer one recommendation and a description of how artemisinin and its derivatives interact with the PARP1 receptor when used as an in silico lung cancer therapeutic agent. This study attempts to uncover and understand the interactions between the active compounds artemisinin and its derivatives and receptors involved in lung cancer cell proliferation by using molecular docking and Molecular Dynamics methods. The molecular docking simulation is an in silico analysis technique that uses a computer to give an overview of how a chemical interacts as a ligand with proteins or receptors in drug discovery studies. Utilizing molecular dynamic simulation, the stability of the binding relationship between the ligand and receptor will be assessed over a specific amount of time. Autodock vina was used for molecular docking simulation. The receptor was taken from the protein database with PDB ID: 7KK6 (PARP1). Molecular Dynamic (MD) simulation using GROMACS 2023 for 100 ns. Interpretation of molecular docking results is shown as affinity values, while the MD results are displayed as RMSD graphs. The binding affinity value can determine the PARP1 receptor and ligand interactions. Low binding affinity values indicate that the protein and ligand binding interactions are becoming more stable. The results of molecular docking showed that artesunate had the most negative binding affinity value of -8.9 kcal/moL, the original ligand (veliparib) was -8.8 kcal/moL, and artemisinin -8.5 kcal/moL, which means that artesunate has the ability binding and mechanism of action similar to veliparib. The RMSD value can be used to assess the binding stability that artemisinin and artesunate create with the PARP1 receptor. RMSD PARP1 with Veliparib has a value of 0.16 nm, while RMSD PARP1 values when interacting with Artesunate and artemisinin are 0.19 and 0.18 nm, respectively. Based on RMSD values and molecular interactions during MD simulations, PARP1 has the same stability when interacting with artesunate, artemisinin, and veliparib. There are similar interactions between veliparib and artesunate and PARP1 is a receptor engaged in the interaction between artemisinin and artesunate on the proliferation of lung cancer cells. Interaction between PARP1 with veliparib and artesunate showed a stable interaction during molecular dynamics simulations. Apart

from normal cells, PARP1 also plays a role in cell cancer. Cancer cells that have been treated with chemotherapy and radiation will make an effort to repair their DNA utilizing PARP1. This situation allows PARP1 to be a target for anticancer treatment.

Keywords: Artemisinin, Artesunate, Lung Cancer, Molecular Docking, PARP1

Introduction

Lung cancer is responsible for about a quarter of cancer fatalities, according to American Cancer Society figures published in 2020. The overall death rate is about 23%, which ranks first, and the incidence of lung cancer and bronchus combined is about 13% (Siegel *et al*., 2018). The treatment of NSCLC (non-small cell lung cancer), a highly invasive malignancy that accounts for around 80% of lung cancers (Saito *et al*., 2017), continues to be complicated. NSCLC is commonly treated with chemotherapy. Conventional chemotherapeutic drugs, on the other hand, frequently induce severe adverse effects. Doxorubicin, for example, can produce significant cardiotoxicity and even heart failure. Platinum-based chemotherapeutic drugs can produce renal and nerve toxicity. Patients with cancer typically receive more than one type of medicine as treatment, which presents the problem of multi-drug resistance. Combination therapy of chemotherapeutic drugs with natural products for tumor treatment is a new method that has shown encouraging outcomes in various studies. This combination therapy will allow the exploration of their use as therapeutic or adjuvant chemotherapeutic agents for the treatment of NSCLC and minimize the adverse effects of chemotherapeutics. Combination therapy, a typical approach in the treatment of cancer, involves the use of various medications to treat a single illness. Combination therapy benefits from synergistic and additive effects since many medications can interact with cancer cells via various molecular pathways, resulting in a more potent anticancer effect and increasing treatment effectiveness.

The shrub-like plant known as *Artemisia* (*Artemisia annua* Linn) is a member of the *Asteraceae* family. The plant is grown in Africa and used as a tea to treat malaria despite originally coming from Asia and Europe. China has a long history of using *Artemisia* as a medicinal plant. Numerous studies have been conducted on artemisia's antimalarial, anticancer, and antioxidant properties. The plant's main antimalarial compound, artemisinin, has been found, and artemisinin derivatives are now recognized as effective antimalarial medications that also work against drug-resistant Plasmodium infections. It contains several essential oil ingredients and artemisinin-related chemicals.

The active ingredient artemisinin, which is isolated from the plant *Artemisia annua* L. (*A. annua*), has been in the spotlight since its discoverer, Youyou Tu, was awarded the Nobel prize in 2015 for the discovery of this chemical as a new malaria cure that was licensed in 1986. Artemisinin and its derivatives (dihydroartemisinin and artesunate) are sesquiterpene lactones with a peroxide group in the form of a 1, 2, 4-trioxane ring structure (Fig. 1). artemisinin and its derivatives have a cytotoxic effect on cancer cells via inhibiting tumor cell proliferation, inducing apoptotic responses, stopping the tumor cell cycle, inhibiting cancer invasion and metastasis, preventing angiogenesis, changing oxidative damage reactions and interfering with cell signalling pathways. More importantly, artemisinin has few adverse effects on normal cells and has been shown to overcome multi-drug resistance in cancer patients.

Inhibiting the Proliferation of Tumor Cells

The interplay of the cell cycle proteins cyclin, Cyclin-Dependent Kinase (CDK), and Cyclin-dependent Kinase Inhibitor (CKI) regulates cell growth and division in healthy cells. However, tumor cells have a significant proliferation potential because of cell mutations, growth signal amplification, impaired testing point regulation, and other factors. Artemisinin and its derivatives can stop the cell cycle in tumor cells, mostly by altering the kinetics of the cell cycle or by disrupting the signalling pathway connected to proliferation (Zhang *et al*., 2018).

Inducing Tumor Cells Apoptosis

Apoptosis is essential for the treatment of tumors. Cancer development and tumor cell drug resistance are likely to be triggered by apoptosis loss or inhibition. One of the most crucial pathways in cell death is the mitochondrial route. When artemisinin and tumor cell ROS interact, the result is a qualitative oxidation of the mitochondrial membrane, an increase in tumor cell ROS, and a decrease in permeability and mitochondrial membrane potential (Noori *et al*., 2014).

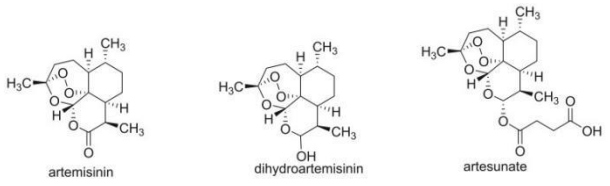

Fig. 1: Chemical structures of artemisinin and its bioactive derivatives

Cell Cycle Arresting

To increase the number of cells that can enter the S phase, tumor cells have the ability to disrupt the G1 to S phase differentiation pathway. Dihydroartemisinin can stop the proliferation of tumor cells by stopping them in the G0/G1 phase. When exposed to dihydroartemisinin, proteins involved in the cell cycle, namely cyclin E, CDK2, and CDK4, were downregulated. Important complexes called Cyclin E, CDK2, and CDK4 guide cells through the G1 phase of the cell cycle and kick off DNA replication. Through boosting the expression of CD71, artemisinin significantly stopped retinoblastoma cells during the G0/G1 and S phases but had little effect on the G2/M phase. More critically, multidrug-resistant retinoblastoma cells can even have their cell cycle arrested by artemisinin (Zhao *et al*., 2013).

Inhibition of Tumor Cell Invasion and Metastasis

Numerous studies have demonstrated that artemisinin and its derivatives can prevent tumor cell invasion and metastasis without regard to the cell line. For instance, in NSCLC, Artesunate can significantly reduce invasion and metastasis. The key processes include suppressing urokinase-type Plasminogen Activator (u-PA) activity protein and mRNA expression, downregulating MMP-2 and MMP-7 mRNA/protein, and upregulating AP-1 and NF-jB transactivation. According to a recent study, the Wnt/b-catenin signalling pathway can be suppressed by the use of artemisinin, dihydroartemisinin, and Artesunate to prevent the invasion and migration of A549 and H1299 cells (Tong *et al*., 2016).

Antiangiogenic Effects

Tumor angiogenesis is primarily characterized by increased vascular permeability, promotion of basal stem cell migration, division and proliferation, acceleration of vessel lumen development, and ultimately, promotion of tumor blood vessel growth via the VEGF receptor released by tumor cells. Therefore, blocking one particular pathway of tumor cell and endothelial cell growth would prevent tumor cell growth and consequently stop the spread of the tumor. Artemisinin and its derivatives can limit tumor cell growth and metastasis by lowering the expression of VEGF and vascular endothelial cell receptors in tumor cells. This prevents new angiogenesis from occurring (Dai *et al*., 2021).

Oxidative Damage Reactions

For their rapid multiplication to continue, tumor cells need more iron. Most experts agree that substances related to artemisinins carry out their antitumor effects through oxidative damage responses. By decreasing the quantity of TfR1 on cell surfaces by an unexpected endocytic pathway, dihydroartemisinin demonstrated a ROS-independent anticancer mechanism. This decreased TfR1-mediated iron uptake resulted in a shortage of cellular iron reserves (Ba *et al*., 2012).

In drug development and pharmacology investigations, the IC_{50} (50% inhibitory concentration equal to one-half of a compound's maximum inhibitory concentration) is most frequently used to calculate pharmacological effectiveness. The IC_{50} number is significant because it shows how much of a drug is required to block a biological process by 50%. Because of an increase in cell mortality or a decrease in cell growth, the IC curves demonstrate a shift in population. Finding the IC_{50} can indicate much more than just reducing cell growth or increasing cell death. Using specific medications at their IC_{50} concentration in cancer results in a 50% reduction in tumor growth. Suppose the IC_{50} is discovered at a lower value during IC curve testing. In that case, this indicates that the drug will be effective at lower concentrations and hence cause less systemic toxicity when administered to patients for therapy. Using the IC_{50} concentration can result in the death of cancer cells and the halting of their proliferation while having a less damaging impact on the body's healthy cells. Artemisinin can inhibit and destroy lung cancer cells, according to clinical trials and *in vitro-in vivo* research. According to research, the IC_{50} values of artemisinin and Artesunate in cell line A549 are 769.60 and 153.54 µm, respectively, with artesunate being more potent than artemisinin. Since IC_{50} values of artemisinin cancer treatment are relatively high, combination therapy can take advantage of the synergistic effect and lower IC_{50} and minimize any dose-related toxicities because combination therapy allows the use of lower doses of multiple agents.

Lung cancer's complicated pathophysiology allows for various avenues to target cancer cells. In this case, once-receptors regulated on the surface of tumor cells, such as Epidermal Growth Factor Receptor (EGFR), Integrin Receptor, Poly ADP Ribose Polymerase (PARP), and others, can be used to inhibit pathways and target more specific cancer drugs. PARP-1 is the most prevalent PARP protein in the nucleus and is involved in various cellular activities, including DNA repair, chromatin remodelling, inflammation, transcriptional control, and cell death. In addition to normal cells, PARP-1 also plays a role in tumor cells. Tumor cells exposed to chemotherapeutic agents and chemoradiation will attempt to repair their DNA using PARP-1. This opens up opportunities for PARP-1 to be used as a target for anticancer therapy. Currently, a PARP inhibitor (PARPi) works as a single agent or is used as adjuvant therapy with chemotherapy and chemoradiation. Although there is evidence of a response, single-agent efficacy is restricted and PARP inhibitors are not currently a part of the therapy options for Small Cell Lung Cancer (SCLC). There is a lot of current research into the mechanisms underlying

these effective therapy combinations, including using PARP inhibitors in treating SCLC. The promise for PARP inhibitor therapy is further supported by the overexpression of PARP1 in SCLC. Byers *et al*. seminal research, which involved unbiased proteomic analysis of cell lines using Reverse-Phase Protein Arrays (RPPA) to find proteins that were differentially expressed in SCLC compared to Non-Small-Cell Lung Carcinoma (NSCLC), was the first to identify PARP as a potential therapeutic target in SCLC (Byers *et al*., 2012).

Several *in vitro* studies have focused on the ability of artemisinin and its derivatives to suppress lung cancer cells. However, many biological processes and mechanisms, such as the interactions between the active compounds (ligands) and receptors, are still poorly understood and require further research. Drug targeting for lung cancer will be more precise, and the inhibition of cancer cell proliferation will be increased due to an understanding of the interaction mechanism between artemisinin and its derivatives with lung cancer receptors. Currently, no studies report the interaction between artemisinin and its derivatives with the PARP1 receptor. The results of this study will offer one recommendation and a description of how artemisinin and its derivatives interact with the PARP1 receptor when used as an in silico lung cancer therapeutic agent. This study attempts to uncover and understand the interactions between the active compounds artemisinin and its derivatives and receptors involved in lung cancer cell proliferation by using molecular docking and molecular dynamics methods.

Materials and Methods

Methods

The flowchart (Fig. 2) represents the method of an in silico analysis of the mechanism of artemisinin and its derivatives as a treatment agent for lung cancer.

The flowchart's specifics are described below:

1. Using the Therapeutic Target database link Database at https://db.idrblab.net, a search for protein receptors related to lung cancer was conducted. Then, in the part search engines, input the disease type, in this case, lung cancer, which will look for target protein receptors
2. The next phase involves using the Cytoscape application version 3.9.1 (https://cytoscape.org) in conjunction with data sources from STITCH: Protein/compound query on the species Homo sapiens to screen for interactions between test ligands and receptors related to lung cancer. In this study, a confidence (score) cutoff of 0.70 is used, while it is advised to use at least 0.50. As the confidence (score) cutoff value approaches 1, it indicates a higher confidence level. Next, the test ligand and all previously grouped receptors are entered into the Cytoscape stitch application to perform a running analysis
3. After the screening results are obtained, proceed with analyzing the properties of protein receptors using Uniprot (https://www.uniprot.org). The analysis includes

a. Availability of 3-dimensional structure properties of protein receptors
b. Availability of reference ligands that bind to
c. protein receptors
d. Has good resolution <2.2 Å

4. Next, the molecular docking process is carried out through the following stages

a. Search and download PARP1 macromolecules The initial stage of this research was to search for the PARP1 macromolecule as a docking target. The search was carried out through the protein data bank via the link https://www.rcsb.org/. The structure with the downloaded identity of 7KK6 is bound to the PARP1 inhibitor ligand (veliparib). The downloaded PARP1 macromolecular data has the identity of 7KK6, which is a dimer (has two chains, namely chain A and chain B) and a resolution of 2.06 Å. The chain used in this research is chain A. The downloaded 7KK6 macromolecule binds to a ligand, namely Veliparib, which is then referred to as the reference ligand
b. Validation: This study's molecular docking method was validated by re-docking the original ligand molecule from the protein that had been downloaded with the PDB code: 7KK6. The parameters used for this validation stage are the Root Mean Square Deviation (RMSD) value and pose, which can be observed visually through the YASARA application. A molecular docking method is said to be valid if the RMSD value is less than 2.0 Å
c. Molecular docking of test compounds and data evaluation: The molecular docking simulation is carried out using plant docking software, and then the docking score is evaluated and compared with Autodock Vina software, which then evaluates the binding affinity. Compared to other molecular docking software (such as Autodock), where a box restricts the molecule, PLANT's boundary is a ball, which is one of the reasons for utilizing it for molecular docking simulations. The benefit of using a grid ball in PLANTS is that when conducting redocking using the same .pdb code, whoever worked on it will get the same results because the software has set it automatically. This is different from

Autodock, where the results of redocking can be obtained differently because each application user creates the grid box independently, so the redocking results will be slightly different

5. Molecular docking results are then verified using Molecular Dynamics (MD) simulations. The molecular dynamics simulation process was carried out to see the stability and flexibility of the binding to the PARP1 receptor after interacting with the ligand. The MD simulation was carried out using the GROMACS application for 100 nanoseconds. Tools and materials

GROMACS

The Groningen machine for chemical simulation is shortened to GROMACS. A unique parallel communication computer system for MD simulations is constructed using this software. Nowadays, the program automatically handles an extensive range of biomolecules, including proteins, lipids, and nucleic acids, which also include built-in force fields for these molecules. In addition to new free-energy methods and several implicit solvent models, GROMACS employs multithreading to achieve effective parallelization even on low-end computers, such as Windows workstations. This offers extraordinarily high performance and cost efficiency when combined with manually adjusted assembly kernels and cutting-edge parallelization for high-throughput and massively parallel simulations.

Amber Tools

Software called Amber is used to simulate MD, particularly with biomolecules. For topology calculations using gmx_MMPBSA and acpype to function, Amber software is needed.

GAFF2

General Amber Force Field 2 (GAFF2) is a force field frequently used in rational drug design. It has parameters for practically all organic molecules composed of C, N, O, H, S, P, F, Cl, Br, and I, and it is compatible with the Amber force field. GAFF2 has the benefit of accounting for hydration, evaporation, free energy, density, and interaction energy.

Acpype

Acpype is a Molecular Mechanics (MM) parameter generator and topology creation program that can compute partial charges. With molecular dynamic simulations like GROMACS, Acpype may generate parameters for tiny compounds that can be used to model protein ligands.

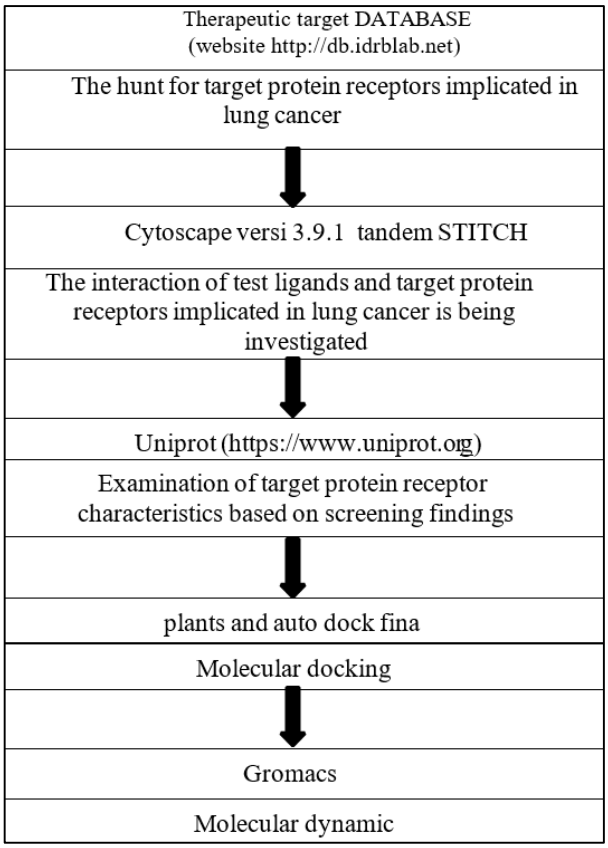

Fig. 2: Flowchart analysis of the mechanism of artemisinin and its derivatives as in silico lung cancer therapeutic agents

Tools

The tools used in this research consist of hardware and software (applications).

The hardware used is as follows:

a. Computer with AMD Ryzen 3 5300U quad-core processor (8 threads), maximum turbo speed 2.6 GHz-3.8 GHz. AMD Chipsets. AMD Radeon RX Vega 7i GPU graphics
b. RAM Memory 8GB LPDDR4x-4266Mhz
c. ASUS ROG GL553 VE series computer with 8GB RAM
d. Computer DELL Optiplex 7000 Tower i9-12900K 64GB
e. 2TB + SSD1TB and Nvidia GeForce RTX 3070 8GB

The software (applications) used are as follows:

a. Plants, Marvin Sketch version 5.2.5.1, YASARA version 19.7.20, notepad++, LigPlot++, Pymol 2.5.4 (64 bit), Chemaxon, Therapeutic Target Database (TTD), CYTOSCAPE version 3.9.1 combined with data sources from stitch, Uniprot and internet connection

b. Autodock Vina integrated into PyRx, discovery studio 2021 client
c. Modeller10.4 running over Chimera1.17.1, GROMACS 2023, AMBER99SB, Acpype

Materials

Materials used:

a. PARP1 receptor was downloaded from the protein data bank (www.rcsb.org) with the identity 7KK6, which binds to the native ligand, namely veliparib. The structure of the PARP1 receptor that binds to its native ligand (Veliparib) is saved in .pdb format
b. The structures of the test ligand compounds, namely artemisinin and Artesunate, were taken from the Canonical SMILE from PubChem database via link https://pubchem.ncbi.nlm.nih.gov/. Pubchem CID code for artemisinin 68827 and for Artesunate 6917864
c. The structures of the test ligand compounds, namely artemisinin and Artesunate, were downloaded from PubChem database via the link https://pubchem.ncbi.nlm.nih.gov/ in sdf format then the ligand is minimized with UFF force field, then converted to pdbqt format
d. Molecular dynamic simulations will be performed using the PARP1 receptor binding complex with the reference ligand and the PARP1 receptor binding complex with the test ligand

Results and Discussion

Analysis of the mechanism of artemisinin and Artesunate compounds as in silico lung cancer therapeutic agents was carried out through the following stages.

The Hunt for Target Protein Receptors Implicated in Lung Cancer

The first step in this investigation was to look for receptors connected to lung cancer. The goal is to identify specific receptors linked to lung cancer. In order to achieve more precise and focused outcomes for in silico research investigating the relationship between lung cancer receptors, test and reference ligands.

Based on the results of the receptor search, lung cancer-related 193 receptors were identified. The 193 receptors were further divided into 10 clusters to facilitate a more straightforward analysis method.

The Interaction of Test Ligands and Target Protein Receptors Implicated in Lung Cancer is Being Investigated

Following identifying the receptors implicated in lung cancer, the next step comprised assessing the receptor-ligand interactions for the three ligands under investigation artemisinin, Artesunate, and dihydroartemisinin, which will be examined in the study. In order to get better and more accurate prediction findings when the molecules are docked, the goal is to identify which lung cancer receptors can interact with the test ligand.

Cytoscape is a software that integrates, visualizes, and analyzes measurement data pertaining to molecular-level network interactions. It is utilized in the screening process. Utilizing Cytoscape software, "component target" and "gene-pathway" networks were constructed. The stitch database, which contains protein network organisms, physical interactions from experimental data and functional linkages via curated pathways, automatic text mining, and prediction approaches, is one of the most popular sources of such networks. However, its web interface is primarily geared toward inspecting tiny networks and the evidence they contain. On the other hand, the Cytoscape software is better suited for working with extensive networks and provides more flexibility in network analysis, data import, and visualization.

A screening process was carried out using Cytoscape software version 3.9.1 (https://cytoscape.org) combined with data sources from STITCH: Protein/compound query on Homo sapiens species. Summary findings of screening the interaction of test ligands and receptors involved in lung cancer from all clusters can be seen in Table 1.

Table 1 reveals that only Artesunate and artemisinin ligands interact with lung cancer receptors, but dihydroartemisinin has no interactions with lung cancer receptors. Artesunate interacts with more receptors in lung cancer than artemisinin. Artemisinin and artesunate may interact with lung cancer receptors because their molecular structure is similar to that of the native ligand, veliparib, which differs from dihydroartemisinin. The presence of this interaction is a promising first sign that the two ligands have potential in the therapy of lung cancer, which the molecular docking procedure will confirm.

Examination of Target Protein Receptor Characteristics Based on Screening Findings

After the screening results, the protein receptor properties were analyzed using Uniprot (https://www.uniprot.org). The analysis includes:

- Presence or absence of 3-dimensional structural properties of protein receptors
- The availability of native ligand binds to a protein receptor
- Has a good resolution, which is < 2.2 Å

Table 1: Screening interaction of test ligand and receptor

No.	Test ligand	Interacting receptors
1	Artesunate	MMP1, VEGFA, ITGB1, PARP1
2	Artemisinin	CDK4
3	Dihydroartemisinin	No interaction with receptors

The 3-dimensional structure of the protein receptor is essential to assess since the docking simulation process will require a 3-dimensional structure to identify suitable active sites on the protein receptor and obtain the best geometry of the ligand-receptor complex. The Protein Data Bank (PDB) contains DNA and other complex molecules that have been published and experimentally determined using X-ray crystallography or NMR spectroscopy.

The presence of original ligands in the form of drugs (particularly lung cancer drugs) that bind to protein receptors is critical in selecting target protein receptors relevant to the research objective, which is to compare the mechanism of action of the test ligand with lung cancer drugs.

The resolution in Uniprot represents the distance between two atomic positions stated in Armstrong, which means that the smaller the Armstrong value, the more exact or detailed the structure obtained.

The summary results of the analysis of the properties of receptors involved in lung cancer and interacting with the test ligands can be seen in Table 2.

Human receptors were used to select the receptors on Uniprot. Only two of the five receptors implicated in lung cancer that interact with test ligands, which are the ITB1 and PARP1 receptors, had native ligands, despite Table 2 above demonstrating that the receptors CDK4, MMP1, VEGFA, ITB1, and PARP1 have good resolution, or <2.2A so that the ITB1 and PARP1 receptors can be used in the molecular docking process.

PARP1_Human was chosen as the target protein receptor model in molecular docking with the PDB code 7KK6 because the ligand bound to the protein is a drug, whereas ITB1_Human's ligand bound to the protein is a glucose derivative, namely NAG: 2-acetamido-2-deoxy-beta-D-glucopyranose. The structure with the identity of 7KK6 was chosen because it is still intact and has not undergone mutations, making it ideal for use as an experimental target. The ligand bound to this macromolecule is veliparib. This PARP1 inhibitor drug can be used as the appropriate positive control for this study.

PARP-1 is the most abundant PARP protein in the cell nucleus and plays a role in various cellular processes. PARP-1 has a size of 116 kD and has 1014 amino acids. Like other members of the PARP family, PARP-1 has a structure with more than one domain that is interconnected in its activity. PARP-1 has a role in several processes in the cell nucleus, including DNA damage repair, chromatin modification, inflammation, transcriptional regulation, and cell death. PARP-1 will bind to DNA, not only to the Single Strand Break (SSB) and Double Strand Break (DSB) damage sites but also to DNA in crossovers, supercoils, and cruciform forms. PARP-1 also has many roles in chromatin modification (Maharani and Wuyung, 2016).

The role of PARP-1 in DNA repair is critical. In addition to normal cells, PARP-1 also plays a role in tumor cells. Tumor cells exposed to chemotherapeutic agents and chemoradiation will attempt to repair their DNA using PARP-1. This opens up opportunities for PARP-1 to be used as a target for anticancer therapy.

Currently, a PARP inhibitor (PARPi) is known which can work as a single agent or be used as adjuvant therapy together with chemotherapy and chemoradiation. The use of PARPi has anti-tumor activity in breast cancer and ovarian cancer with BRCA-1 and/or BRCA-2 mutations (Maharani and Wuyung, 2016; Fong *et al*., 2009).

Veliparib is a potent oral PARP-1 and PARP-2 inhibitor and has demonstrated antitumor activity, both as monotherapy and in combination with other chemotherapeutics such as platinum-based agents in preclinical models and in patients with solid tumors (Govindan *et al*., 2022).

Molecular Docking

Previous studies employing the molecular docking simulation method have investigated the anti-lung cancer activity of the *Artemisia annua* plant. The EGFR receptor (PDB ID: 2ITP, 2ITY, 2J5F, 4I23, 4JHO) was engaged in this investigation. Using PLANT's software to compare the score values of the native ligands, erlotinib and coumarin, against the validated EGFR receptor and MOE software to visualize the docking results, the docking data analysis was completed. Coumarin derivative molecules had greater docking scores than native ligands and erlotinib, according to test results on the five PDB codes. The amino acids that bind to native ligands and erlotinib in the EGFR receptor can also be bound by coumarin derivative molecules. However, the binding of coumarin derivatives to the EGFR receptor is less stable, so coumarin derivative compounds are not antagonists to the EGFR receptor (Ticia, 2020). The binding of the original ligand, Veliparib, to the PARP1 receptor, validates the molecular docking method employed as a reference using PLANTS software. The RMSD value obtained from PDB code 7KK6 is 0,6491Å (< 2.0Å), and the resulting pose is close to the native conformation. The validation findings confirm that the PDB code is correct and can be utilized in the next docking step. The prepared ligands were then docked to the previously validated protein. The docking score between the test ligand and the reference ligand for the PARP1 receptor can be seen in Table 3 as follows.

Table 2: Analysis properties of lung cancer receptors

No.	Target Protein Receptors	Classifications	Number of PDB Codes, with resolution < 2,2Å	Number of PDB codes whose protein receptors have native ligands
1	CDK4_human	Cell cycle, transferase	5	None of the native ligands attach to the receptor
2	MMP1_human	Hydrolase/metalloprotease	10	None of the native ligands attach to the receptor
3	VEGFA_Human	Hormone/Growth factor/immune SYSTEM/transferase/transport protein/signalling protein/Peptide binding protein	42	None of the native ligands attach to the receptor
4	ITB1_human	Cell Adhesion/immune system	9	6
5	PARP1_human	Transferase/transferase inhibitor/ antitumor protein	63	50

Table 3: Docking score between the test ligand and the reference ligand for the PARP1 receptor

No.	PDB Code	Ligand	Docking score
1	7KK6 RMSD 0,6491Å	Veliparib	-98,41
		Artemisinin	-75,76
		Artesunat	-92,28

Table 3 above, it can be seen that the docking score of the reference ligand Veliparib is lower than that of the artemisinin and Artesunate compounds. Based on this, it can be said that the bond complex between the protein and the native ligand is the most stable, followed by the bond complex between the protein and the Artesunate ligand. Meanwhile, the binding complex between the protein and artemisinin is less stable when compared to the Veliparib and Artesunate ligands. However, the main goal of this research is not to find an active compound that can replace Veliparib as a lung cancer drug. However, to search for and understand the mechanism of interaction between the active compounds artemisinin and Artesunate and receptors involved in lung cancer cell growth using the molecular docking method, where artemisinin and Artesunate compounds have been shown *in vitro* to be able to inhibit cancer cell growth lungs.

Artemisinin and Artesunate compounds can interact with binding sites on the PARP1 receptor by binding to their amino acids. The amino acids that bind to artemisinin and Artesunate can bind to some of the same amino acids as those that bind to the Veliparib ligand. The binding complex between the native ligand (Veliparib) and PARP1 is better when compared to artemisinin and artesunate. There are similarities in interactions with Veliparib, artemisinin, and Artesunate, where all three interact with two critical amino acid residues of PARP1, namely Gly863 and His862, through hydrogen bonds.

Molecular Dynamic

Process Molecular Dynamics (MD) Simulation was carried out to see the stability of the bond in PARP1 after interacting with the ligand. The MD process was carried out using GROMACS software (Abraham *et al*., 2015). The software reads an error notification while generating a protein topology using the Amber force field (Lindorff-Larsen *et al*., 2010). Because the mistake read is a missing amino acid sequence, the amino acid sequence must first be rectified using Modeller 10.4 and Chimera 1.17.1 (Eswar *et al*., 2008). Before the refined protein is used for docking, its quality is validated using the PSVS (Protein Structure Validation Software) application, which looks to see if there is a difference in the protein structure quality before and after refinement. The refined protein's quality was assessed by comparing the Ramachandran plot score before and after refining (Table 4).

Table 4 shows no difference in the protein structure quality before and after refinement (in fact, there is slight improvement in protein structure after refinement). Verification of the protein's 3D structure before and after refinement revealed no differences, implying that the quality of the protein structure before and after refinement was the same and could be used for the docking process based on the results of the protein structure validation. Furthermore, utilizing Autodock Vina software, the protein docking procedure with ligands was continued (Dallakyan and Olson, 2015).

Redocking was carried out between PARP1 and veliparib to validate the docking results. Grid docking Center X = -9.2460, Y = -4.3584, Z = 7.2795; Dimensions X = 15.4106, Y = 16.4510, Z = 14.7887. From the redocking results, an RMSD of 1.2527 Å was obtained. The RMSD value of the redocking result is less than 2 Å, indicating that the docking result is valid so that it can be continued for the docking process of the test compound. From the docking results, the Artesunate test ligand had the most negative binding affinity value of -8.9 kcal/moL. However, there was only a slight difference from the native ligand (Veliparib), which was -8.8 kcal/moL, followed by the artemisinin test ligand -8.5 kcal/moL. The docking results produced with the Autodock Vina software match those acquired with the plants software, indicating that the resultant interactions are the same.

Table 4: The results of protein validation before and after PSVS refining

Ramachandran plot summary from Procheck (most favored region)		Ramachandran plot statistic from Richardson's lab (most favored region)		Verify 3D	
Before Refinement	After refinement	Before refinement	After refinement	Before refinement	After refinement
91,3%	91,6%	98,1%	98,9%	0,24	0,28

This study uses molecular docking to select compounds with the highest affinity and make a stable interaction by identifying the orientation between the ligand and the PARP1 receptor. The Gibbs free energy is used to calculate the stability properties. If a ligand has a higher affinity for a protein, the ligand-receptor bond complex will be more stable. Conversely, if the docking score is higher, the affinity will be lower, and the ligand-receptor bond complex will be more unstable. The binding affinity of the test ligand artesunate is similar to that of the reference ligand veliparib. This indicates that artesunate has binding stability comparable to veliparib and may have lung anticancer properties, supporting the findings of both *in vitro* and *in vivo* experiments.

The bond interactions are formed as hydrogen bonds or other bonds that influence each other, such as van der Waals interactions and other interactions. In the binding of Veliparib with the PARP1 receptor, it can be seen that several interactions occur, including four hydrogen bonds that occur in the polyprotein A chain with the amino acid residues TRP202, GLY204, TYR237, and SER245. Other bonds formed are hydrophobic bonds (in the form of van der Waals interactions, pi-sigma bonds, and pi-alkyl bonds). The interaction that occurs in the docking of the Artesunate compound with the PARP1 receptor is almost the same as the interaction that occurs in the docking of the original ligand, where three hydrogen bonds occur in the polyprotein A chain with the amino acid residues HIS203, SER245 and TYR248. Another bond that is formed is hydrophobic.

Meanwhile, the artemisinin test ligand did not show any hydrogen bond interactions, but there were other bond interactions, namely pi-Alkyl and pi-Sigma. There is a similar interaction between veliparib and artesunate, where both interact with one critical amino acid residue of PARP1, namely SER245, through hydrogen bonds. Ligand superimposes from the results of the molecular docking simulation between veliparib (blue), artesunate (red), and artemisinin (green) can be seen in Fig. 3. Superimposition also specifies the optimal ligand structural pose, as shown in the compounds that overlap between the test and reference ligands. According to the overlaid data, the Artesunate ligand has a pose conformation similar to the veliparib ligand. In contrast, the artemisinin ligand has a pose conformation significantly distinct from the Veliparib ligand on the 7KK6 receptor protein (Fig. 3). This is consistent with the docking studies, which show that Artesunate and Veliparib have similar binding affinity for the 7KK6 receptor protein when compared to the artemisinin ligand. This suggests the artesunate compound has the exact anti-lung cancer mechanism as the comparative chemical veliparib.

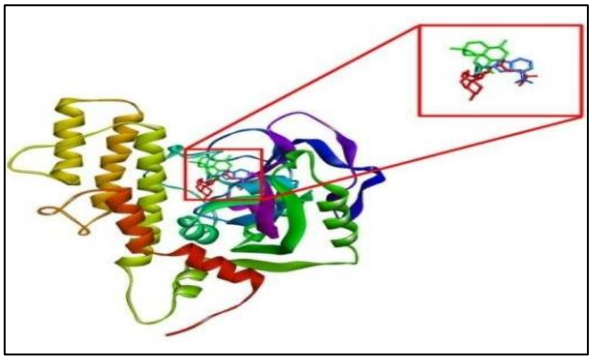

Fig. 3: Ligand superimpose of molecular docking veliparib, artesunate, and artemisinin

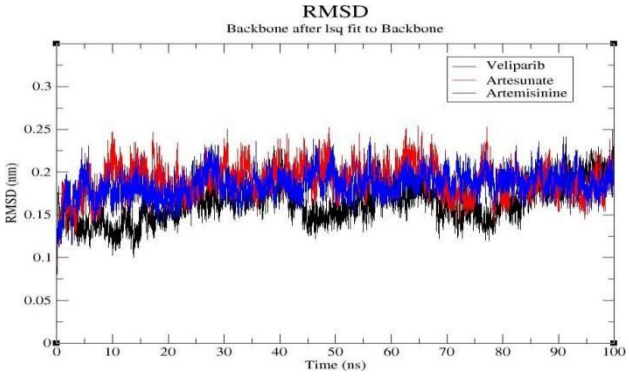

Fig. 4: RMSD PARP1 with the ligands

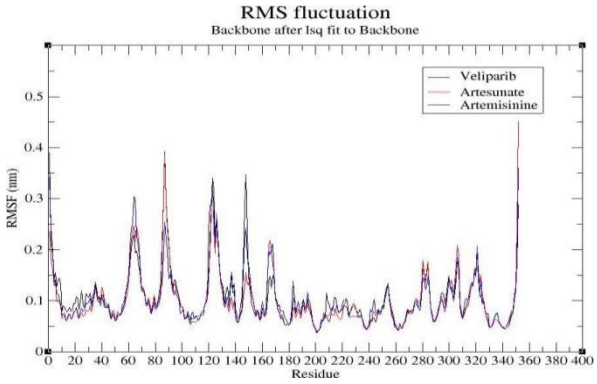

Fig. 5: RMSF PARP1 with the ligands

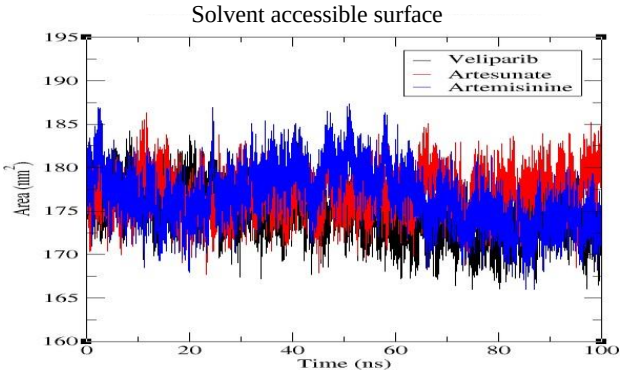

Fig. 6: RMSF PARP1 with the ligands

Molecular Dynamic (MD) Simulation of complex molecular docking results is evaluated with the RMSD (Root Mean Square Deviation) parameter. The alterations and migrations of compounds in protein active pockets were measured using RMSD measurements for each frame. A molecular dynamics simulation was carried out for (100 ns) to see the stability of PARP1 after interacting with the ligand. RMSD PARP1 with control ligand (veliparib) has a value of 0.16 nm. Meanwhile, the RMSD values for PARP1 when interacting with Artesunat and artemisinin were 0.19 and 0.18 nm, respectively, as shown in Fig. 4. This value indicates a slight increase in RMSD. However, the RMSD value is still less than 1. This indicates that PARP1 has the same stability when interacting with the test ligand and veliparib.

The flexibility of the PARP1 protein complex with ligands (Fig. 5) was examined in addition to the RMSD value. The mean square deviation of each amino acid residue from its starting position is determined by Root Mean Square Fluctuation (RMSF) analysis, which shows how flexible or rigid a protein is in different areas. The flexibility of the residue during pressure treatment increases with residual variation (Huang *et al*., 2021). This study determined the average flexibility of the target proteins using this method. When interacting with veliparib and artesunate, the GLY204 and SER245 residues exhibited no modifications. In the meantime, the two significant residues of artemisinin do not form hydrogen bonds.

To observe the interaction between PARP1 and the ligand, shooting was performed at 1ns (start), 50ns (middle), and 100 ns (end) of the simulation shown in Fig. 7. During the molecular dynamic simulation, the interaction between PARP1 and veliparib and artesunate demonstrated a stable contact with GLY204 and SER245 residues. This shows that artesunate may be able to bind to PARP1 stably. On the other hand, artemisinin did not interact with the two residues. Protein's solvent-accessible surface area, or SASA, is an important concern in protein folding and stability research. SASA measures the surface area of a biomolecule (such as a protein) or other molecular structure accessible to solvent molecules. It is the maximum extent to which atoms on a protein surface can come into contact with the solvent and is measured in squared nanometers (nm^2). SASA is a quantity that is very important in functional research and protein folding. It is frequently used in protein computational studies and is critical to understanding the structure-function relationship of proteins and their residues. For example, hydrophobic residue burial can play a significant role in the folding of proteins, and the stability of the protein is directly correlated with the exposure of these residues to the hydrophobic core and solvent.

Relative growth may be indicated by an increase in SASA values (Krebs and De Mesquita, 2016). The SASA value was 174.2 nm^2 when PARP1 interacted with veliparib. At the same time, it was 176.9 nm^2 and 176.3 nm^2 when PARP1 interacted with Artesunat and artemisinin (Fig. 6). When compared to native protein, a higher SASA value denotes easier access to the PARP1 surface.

Based on RMSD values and molecular interactions during molecular dynamic simulations, artesunate has similar capabilities to veliparib. Thus, artesunate likely has the same ability as native ligands to bind to PARP1 and provide a similar mechanism of action and pharmacological effects.

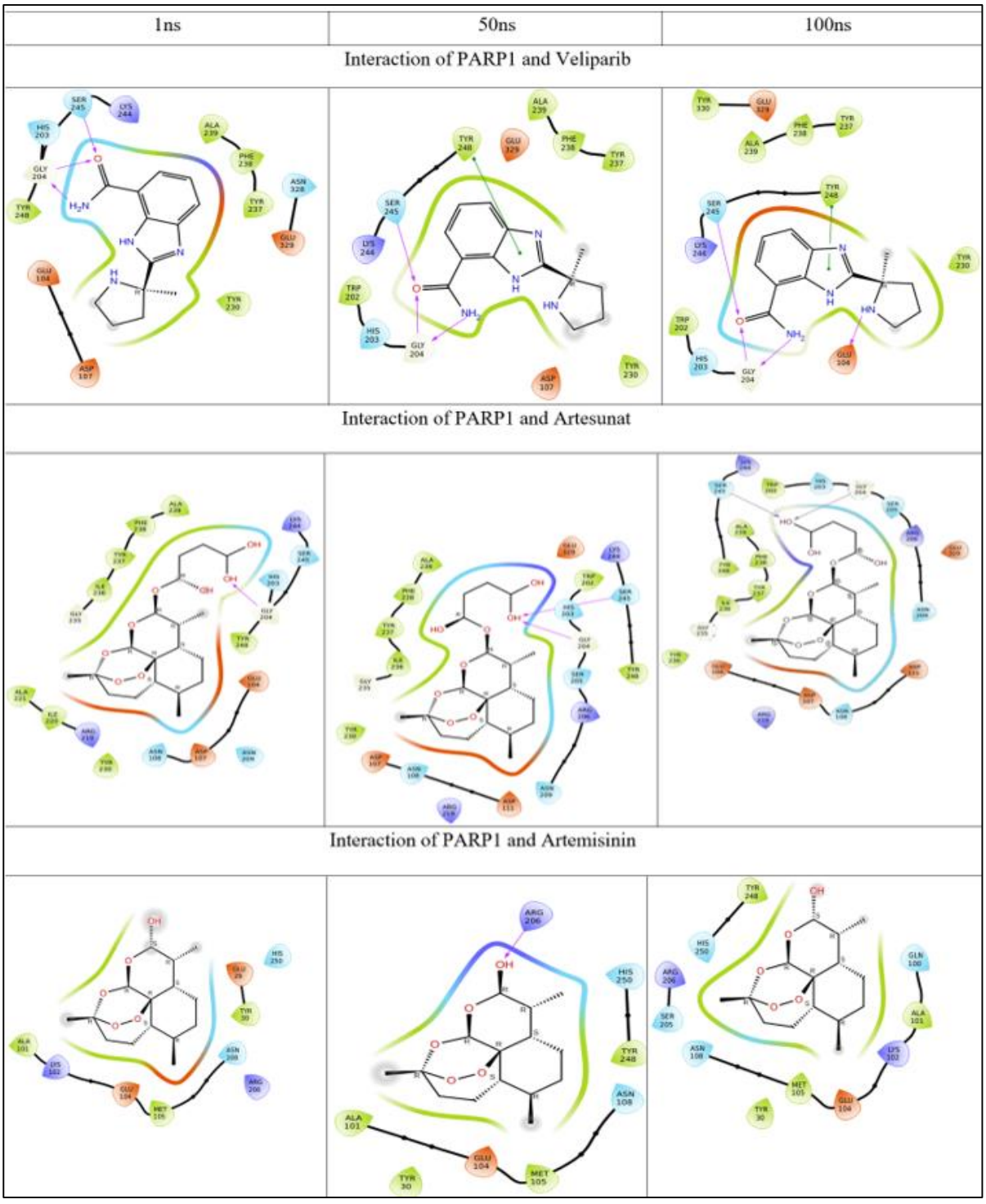

Fig. 7: Interaction between PARP1 and the ligand at 1ns (start), 50 ns (middle) and 100 ns (end

Conclusion

1. PARP1 is the target protein receptor that interacts with the active chemicals artemisinin and artesunate in developing lung cancer cells. Veliparib and artesunate have a similar interaction in that they interact with one crucial amino acid residue of PARP1, SER245, via hydrogen bonding. Meanwhile, no hydrogen interactions with critical amino acid residues were seen with artemisinin. Molecular

dynamic simulations reveal a stable interaction between PARP1, veliparib, and artesunate with GLY204 and SER245 residues. This shows that artesunate may be able to bind to PARP1 persistently. Meanwhile, artemisinin did not interact with the two residues.

Acknowledgment

The authors would like to express gratitude to Atma Jaya Catholic University of Indonesia for the financial support.

Funding Information

The authors have not received any financial support or funding to report.

Author's Contributions

Didik Harmoko: Perform data collection and data analysis. Written the drafted and revised manuscript.

Vivitri Dewi Prasasty and Adi Yulandi: Advised, giving feedback, and engage in dialogue while drafted and revised manuscript.

Ethics

This article is original and contains unpublished material. The corresponding author confirms that all of the other authors have read and approved the manuscript and that no ethical issues are involved.

References

Abraham, M. J., Murtola, T., Schulz, R., Páll, S., Smith, J. C., Hess, B., & Lindahl, E. (2015). GROMACS: High performance molecular simulations through multi-level parallelism from laptops to supercomputers. *SoftwareX*, *1*, 19-25. https://doi.org/10.1016/j.softx.2015.06.001

Ba, Q., Zhou, N., Duan, J., Chen, T., Hao, M., Yang, X., Li, J., Yin, J., Chu, R., & Wang, H. (2012). Dihydroartemisinin exerts its anticancer activity through depleting cellular iron via transferrin receptor-1. https://doi.org/10.1371/journal.pone.0042703

Byers, L. A., Wang, J., Nilsson, M. B., Fujimoto, J., Saintigny, P., Yordy, J., Giri, U., Peyton, M., Fan., Y., Diao, L., Masrorpour, F., Shen, L., Liu, W., Duchemann, B., Tumula, P., Bhardwaj, V., Welsh, J., Weber, S., Glisson, B., Kalhor, N., Ignacio, I., Girard, L., Lippman, S., Mills, G., Coombes, K., Weinstein, J., Minna, J., & Heymach, J. V. (2012). Proteomic profiling identifies dysregulated pathways in small cell lung cancer and novel therapeutic targets including PARP1. *Cancer Discovery*, *2*(9), 798-811. https://doi.org/10.1158/2159-8290.CD-12-0112

Dai, X., Zhang, X., Chen, W., Chen, Y., Zhang, Q., Mo, S., & Lu, J. (2021). Dihydroartemisinin: A potential natural anticancer drug. *International Journal of Biological Sciences*, *17*(2), 603. https://doi.org/10.7150/ijbs.50364

Dallakyan, S., & Olson, A. J. (2015). Small-molecule library screening by docking with PyRx. *Chemical biology: Methods and Protocols*, 243-250. https://doi.org/10.1007/978-1-4939-2269-7_19

Eswar, N., Eramian, D., Webb, B., Shen, M. Y., & Sali, A. (2008). Protein structure modeling with MODELLER. *Structural proteomics: High-Throughput Methods*, 145-159. https://doi.org/10.1007/978-1-60327-058-8_8

Fong, P. C., Boss, D. S., Yap, T. A., Tutt, A., Wu, P., Mergui-Roelvink, M., Mortimer, P., Swaisland, H., Lau, A., O'Connor, M., Ashworth, A., Carmichael, J., Kaye, S.B., Schellens, & De Bono, J. S. (2009). Inhibition of poly (ADP-ribose) polymerase in tumors from BRCA mutation carriers. *New England Journal of Medicine*, *361*(2), 123-134. https://doi.org/10.1056/NEJMoa0900212

Govindan, R., Lind, M., Insa, A., Khan, S. A., Uskov, D., Tafreshi, A., Guclu, S., Bar, J., Kato, T., Lee, H., K., Nakagawa, K., Hanse, O., Biesma, B., Kundu, M., G., Dunbar, M., He, L., Ansell, P., Sehgal, V., Huang, X., Glasgow, J., & Bach, B. A. (2022). Veliparib Plus Carboplatin and Paclitaxel Versus Investigator's Choice of Standard Chemotherapy in Patients with Advanced Non-Squamous Non-Small Cell Lung Cancer. *Clinical Lung Cancer*, *23*(3), 214-225. https://doi.org/10.1016/j.cllc.2022.01.005

Huang, Y., Zhang, X., & Suo, H. (2021). Interaction between β-lactoglobulin and EGCG under high-pressure by molecular dynamics simulation. *Plos One*, *16*(12), e0255866. https://doi.org/10.1371/journal.pone.0255866

Krebs, B. B., & De Mesquita, J. F. (2016). Amyotrophic lateral sclerosis type 20-In Silico analysis and molecular dynamics simulation of hnRNPA1. *PloS One*, *11*(7), e0158939. https://doi.org/10.1371/journal.pone.0158939

Lindorff-Larsen, K., Piana, S., Palmo, K., Maragakis, P., Klepeis, J. L., Dror, R. O., & Shaw, D. E. (2010). Improved side-chain torsion potentials for the Amber ff99SB protein force field. *Proteins: Structure, Function and Bioinformatics*, *78*(8), 1950-1958. https://doi.org/10.1002/prot.22711

Maharani, M. A. P., & Wuyung, P. E. (2016). Peran Poly (ADP-ribose) Polymerase-1 pada Perbaikan Kerusakan DNA. *Pratista Patologi*, *5*(1), 1-9.

Noori, S., Hassan, Z. M., & Farsam, V. (2014). Artemisinin as a Chinese medicine, selectively induces apoptosis in pancreatic tumor cell line. *Chinese Journal of Integrative Medicine*, *20*, 618-623. https://doi.org/10.1007/s11655-013-1454-2

Saito, S., Espinoza-Mercado, F., Liu, H., Sata, N., Cui, X., & Soukiasian, H. J. (2017). Current status of research and treatment for non-small cell lung cancer in never-smoking females. *Cancer Biology and Therapy*, *18*(6), 359-368. https://doi.org/10.1080/15384047.2017.1323580

Siegel, R. L., Miller, K. D., & Jemal, A. (2018). Cancer statistics, 2018. *CA: A Cancer Journal for Clinicians*, *68*(1), 7-30. https://doi.org/10.3322/caac.21442

Ticia, W. (2020). *Molecular Docking Senyawa Turunan Kumarin Pada Tanaman Artemisia (Artemisia annua L.) Terhadap Reseptor Egfr Sebagai Kandidat Antikanker Paru-Paru* (Bachelor Degree thesis, Universitas Wahid Hasyim). https://eprints.unwahas.ac.id/2748/

Tong, Y., Liu, Y., Zheng, H., Zheng, L., Liu, W., Wu, J., Ou, R., Zhang, G., Li, F., Hu, M., Liu, Z., & Lu, L. (2016). Artemisinin and its derivatives can significantly inhibit lung tumorigenesis and tumor metastasis through Wnt/β-catenin signaling. *Oncotarget*, *7*(21), 31413. https://doi.org/10.18632/oncotarget.8920

Zhang, Y., Xu, G., Zhang, S., Wang, D., Saravana Prabha, P., & Zuo, Z. (2018). Antitumor research on artemisinin and its bioactive derivatives. *Natural Products and Bioprospecting*, *8*, 303-319. https://doi.org/10.1007/s13659-018-0162-1

Zhao, F., Wang, H., Kunda, P., Chen, X., Liu, Q. L., & Liu, T. (2013). Artesunate exerts specific cytotoxicity in retinoblastoma cells via CD71. *Oncology Reports*, *30*(3), 1473-1482. https://doi.org/10.3892/or.2013.2574